NIH Public Access
Author Manuscript
Cell Stem Cell. Author manuscript; available in PMC 2013 April 13.

Published in final edited form as:
Cell Stem Cell. 2011 January 7; 8(1): 72–83. doi:10.1016/j.stem.2010.11.030.

Robo4 Cooperates with Cxcr4 to Specify Hematopoietic Stem Cell Localization to Bone Marrow Niches

Stephanie Smith-Berdan[1], **Andrew Nguyen**[1], **Deena Hassanein**[1], **Matthew Zimmer**[1], **Fernando Ugarte**[1], **Jesús Ciriza**[2], **Dean Li**[3], **Marcos E. García-Ojeda**[2], **Lindsay Hinck**[1], and **E. Camilla Forsberg**[1,*]

[1]Institute for the Biology of Stem Cells, University of California Santa Cruz, Santa Cruz, CA 95064, USA

[2]School of Natural Sciences, University of California Merced, Merced, CA 95343, USA

[3]Department of Oncological Sciences, University of Utah, Salt Lake City, UT 84112, USA

Summary

Specific bone marrow (BM) niches are critical for hematopoietic stem cell (HSC) function during both normal hematopoiesis and in stem cell transplantation therapy. We demonstrate that the guidance molecule Robo4 functions to specifically anchor HSCs to BM niches. Robo4-deficient HSCs displayed poor localization to BM niches and drastically reduced long-term reconstitution capability while retaining multilineage potential. Cxcr4, a critical regulator of HSC location, is upregulated in *Robo4*$^{-/-}$ HSCs to compensate for Robo4 loss. Robo4 deletion led to altered HSC mobilization efficiency, revealing that inhibition of both Cxcr4- and Robo4-mediated niche interactions are necessary for efficient HSC mobilization. Surprisingly, we found that WT HSCs express very low levels of Cxcr4 and respond poorly to Cxcr4 manipulation relative to other hematopoietic cells. We conclude that Robo4 cooperates with Cxcr4 to endow HSCs with competitive access to limited stem cell niches, and we propose Robo4 as a therapeutic target in HSC transplantation therapy.

Introduction

The tremendous potential of stem cells to provide a complete and permanent cure for a wide range of human disorders makes progress in improving the safety and efficiency of cell-based therapies a top priority in modern medicine. Successful hematopoietic cell transplantations have been performed for more than 50 years and have made HSCs the paradigm for stem cell therapy. Still, the morbidity and mortality of hematopoietic transplant recipients are unacceptably high and transplants are therefore reserved for patients with few other treatment options. By investigating the molecular mechanisms of HSC interaction with the bone marrow (BM) microenvironment, our goal is to enable specific and efficient manipulation of both HSC mobilization and engraftment.

Because mobilized peripheral blood (PB) is an increasingly common source of HSCs, transplantation therapy involves HSC movement both into and out of the BM. In mice, as well as in humans, combined administration of cytoxan (cyclophosphamide) and G-CSF (Cy/G treatment) induces self-renewing divisions of BM HSCs, resulting in an expansion of

©2011 Elsevier Inc.

*Correspondence: cforsber@ucsc.edu.

Supplemental Information: Supplemental Information includes Supplemental Experimental Procedures and six figures and can be found with this article online at doi:10.1016/j.stem.2010.11.030.

NIH-PA Author Manuscript
NIH-PA Author Manuscript
NIH-PA Author Manuscript

NIH-PA Author Manuscript

NIH-PA Author Manuscript

NIH-PA Author Manuscript

the HSC pool followed by migration of HSCs to the blood stream (Morrison et al., 1997; Passegué et al., 2005; Wright et al., 2001). More recently, AMD3100, an antagonist of the G protein-coupled receptor Cxcr4, has been used to mobilize hematopoietic cells (Broxmeyer et al., 2005; Liles et al., 2003; Watt and Forde, 2008). In contrast to Cy/G, AMD3100-induced mobilization is rapid, with increased numbers of progenitors detected in the blood 1 hr after administration of a single dose of drug, and thus does not involve cell expansion. Upon transplantation, intravenously injected HSCs must find their way back to the BM and engraft. Most likely, HSCs home in response to chemokines, including the Cxcr4 ligand Sdf1 (also known as Cxcl12), followed by adhesion to the niche by engaging in specific interactions with cellular and matrix components. Engraftment of transplanted HSCs requires partial or complete myeloablation to allow donor HSCs access to HSC-supportive niches. The ability to long-term engraft is a defining and unique property of HSCs and critically important for both normal hematopoietic development and transplantation therapy.

Sdf1 and Cxcr4 play pivotal roles in HSC location and function. Mice deficient in either Sdf1 or Cxcr4 die during late embryogenesis and lack BM hematopoiesis (Nagasawa et al., 1996; Zou et al., 1998). As described above, the Cxcr4 antagonist AMD3100 can be used to mobilize hematopoietic progenitors from the BM to PB in mice and humans (Broxmeyer et al., 2005; Watt and Forde, 2008), and Cxcr4-blocking antibodies impair HSC engraftment (Peled et al., 1999). In addition, HSCs actively migrate toward Sdf1 in transwell migration assays (Lapidot, 2001; Wright et al., 2002), and recent data suggest that HSCs specifically localize next to BM cells expressing high levels of Sdf1 (Sugiyama et al., 2006). Thus, there is extensive evidence supporting critical roles for Sdf1 and Cxcr4 in regulating HSC location.

Surprisingly, however, deletion of Cxcr4 in adulthood results in HSCs capable of homing and engraftment (Nie et al., 2008; Sugiyama et al., 2006). In addition, many cells other than HSCs express Cxcr4, making it unlikely that Cxcr4, alone, specifies HSC location to stem-cell-supportive niches. In search of HSC-specific receptors capable of specifying cell location, we recently identified the single-transmembrane receptor Robo4 on HSCs by gene expression microarray analysis (Forsberg et al., 2005). A subsequent report confirmed that Robo4 marks long-term reconstituting HSCs (Shibata et al., 2009). Robo4, like its family members Robo1-3, is capable of regulating cell location by responding to the Slit family of secreted ligands (Kaur et al., 2006; Park et al., 2003; Seth et al., 2005; Suchting et al., 2005). Other than HSCs, Robo4 expression seems restricted to endothelial cells, where it functions to regulate blood vessel sprouting (Huminiecki et al., 2002; Park et al., 2003). *Robo4*$^{-/-}$ mice, though grossly normal, have defects in VEGF- and Slit-induced regulation of vascular integrity and angiogenesis (Jones et al., 2008; London et al., 2010; Marlow et al., 2010). Here, we show that Robo4 acts as an HSC-specific adhesion molecule that cooperates with Cxcr4 to localize HSCs to BM niches.

Results

Robo4 Expression Is Restricted to HSCs Tightly Associated with BM Niches

Our previous gene expression microarray analysis showed that Robo4 is expressed at higher levels by HSCs compared to MPP, Cy/G-mobilized HSCs (M-HSCs), and leukemic HSCs (L-HSCs) (Forsberg et al., 2005, 2010). We verified these results by qRT-PCR and extended the analysis to include multiple BM cell types representing the major hematopoietic progenitor populations and lineages. We found that Robo4 is very selectively expressed by HSCs and downregulated upon differentiation and mobilization and in leukemogenesis (Figures 1A and 1B). Substantial numbers of M-HSCs and L-HSCs are found in the blood, spleen, and liver (Morrison et al., 1997; Passegué et al., 2004), so Robo4 downregulation may facilitate exit from HSC niches in the BM. Intriguingly, Robo4 transcripts were barely

NIH-PA Author Manuscript

NIH-PA Author Manuscript

NIH-PA Author Manuscript

detectable in fetal liver HSCs and increased significantly in BM HSCs during fetal to adult development (Figure 1C), further emphasizing the specificity of Robo4 expression to HSCs located in the BM. Cell surface staining via a monoclonal antibody specific for Robo4 (Figure 1E) showed that Robo4 protein is robustly expressed by all adult BM HSCs, with lower levels on ST-HSCs and MPP, and absent from other hematopoietic cell types (Figure 1D; for flow cytometry gating strategies see Figure S1A available online), in agreement with the qRT-PCR data (Figure 1A). Less than 1% of total nucleated BM cells are Robo4 positive, so Robo4 is an excellent HSC-specific marker.

Because different Robo receptors may be functionally redundant, we also analyzed the expression of Robo1, 2, and 3. Previous studies have reported that circulating hematopoietic cells express Robo1 and respond to the Robo ligand Slit2 (Prasad et al., 2007; Wu et al., 2001). In addition, it has been suggested that Robo4 heterodimerization with Robo1 is required for Robo4 response to Slits (Sheldon et al., 2009). However, we did not detect robust expression for either Robo1, 2, or 3 in purified hematopoietic cell populations by using qRT-PCR under conditions that readily detected these transcripts in brain tissue (data not shown). Additionally, we were unable to detect Robo1 on any BM or PB cell type, including HSCs, by flow cytometry by means of a monoclonal antibody that detected Robo1 on WT, but not *Robo1*$^{-/-}$, brain cells (Figure S1B). These data are consistent with a recent report (Shibata et al., 2009) and suggest that Robo4 is the predominant Robo receptor on hematopoietic cells. Importantly, Robo4 expression is restricted to HSCs that maintain tight interactions with the BM niche.

Reduced BM Interaction of HSCs Lacking Robo4

To assess the functional role of Robo4 in vivo, we analyzed the frequencies of hematopoietic cells in the BM, spleen, and blood of Robo4-deficient mice. Strikingly, analysis of cell frequencies in the BM under normal, nonstress conditions revealed that *Robo4*$^{-/-}$ mice displayed a significant decrease in HSC frequencies, whereas other cell types were not affected (Figure 2A). This decrease in HSC BM frequencies was mirrored by a reproducible increase in HSC frequencies in PB (Figure 2B). HSC numbers in the spleen were not affected (Figure S2A). To test whether the decrease in HSC BM frequencies reflects defects in HSC proliferation, we assayed proliferative activity in vitro and in vivo. We detected no differences in the cell cycle status of *Robo4*$^{-/-}$ HSCs or progenitors compared to WT mice (Figures S2B and S2C). We also tested the in vitro expansion rates of WT and *Robo4*$^{-/-}$ HSCs, and whether the putative Robo4 ligand Slit2 elicits a proliferative response on WT HSCs, without detecting significant differences (Figures S2D and S2E). Consistent with these data, *Robo4*$^{-/-}$ HSCs were as able as WT HSCs to restore hematopoiesis after weekly injections of the cytotoxic agent 5-fluoro-uracil (5-FU) (Figure S2F). Thus, loss of Robo4 does not significantly impair HSC proliferative capacity. Lower HSC frequencies in *Robo4*$^{-/-}$ BM may instead be explained by reduced HSC retention in the BM. This is supported by the HSC increase in PB in *Robo4*$^{-/-}$ mice (Figure 2B) and also by downregulation of Robo4 in M-HSCs and L-HSCs (Figure 1B) as mobilization and leukemia lead to higher numbers of HSCs in the PB, spleen, and liver (Morrison et al., 1997; Passegué et al., 2004).

Robo4$^{-/-}$ HSCs Display Poor BM Engraftment, but Normal Differentiation Capacity

To test whether Robo4 plays a role in HSC reconstitution of hematopoiesis upon transplantation, we competitively transplanted 100 HSCs from WT and *Robo4*$^{-/-}$ mice into congenic hosts and monitored PB cell readout for 16 weeks. *Robo4*$^{-/-}$ HSCs performed as well as WT HSCs up to 3 weeks, but failure to provide sustained hematopoietic expansion over time resulted in a significant difference in PB cell readout beyond 6 weeks (Figure 2C). The ratios of mature myeloid, B, and T cells were not significantly affected by the loss of

NIH-PA Author Manuscript

NIH-PA Author Manuscript

NIH-PA Author Manuscript

Robo4 (Figure 2D). Interestingly, we detected no differences between WT and *Robo4*$^{-/-}$ HSCs in in vivo spleen colony-forming assays (CFU-S_{12}) (Figure 2E), indicating that the impaired transplantation defect is specific for the BM. Indeed, analysis of the BM of long-term reconstituted animals revealed significantly fewer *Robo4*$^{-/-}$ HSCs compared to WT HSCs (Figure 2F). These data show that *Robo4*$^{-/-}$ HSCs display a specific and significantly impaired ability to engraft in the BM. However, the *Robo4*$^{-/-}$ HSCs that do engraft are maintained over time and produce normal ratios of mature cells.

HSCs Lacking Robo4 Mobilize Less Efficiently with Cy/G Treatment

Decreased BM frequencies at steady-state (Figure 2A) and impaired BM engraftment (Figures 2C and 2E) of *Robo4*$^{-/-}$ HSCs suggest that Robo4 mediates adhesive interactions between HSC and BM niches. Consequently, Robo4 downregulation upon Cy/G-induced mobilization (Figure 1B) may be necessary for efficient HSC relocation from BM to PB. We therefore hypothesized that *Robo4*$^{-/-}$ HSCs would be mobilized with greater efficiency compared to WT HSC. To test this directly, we subjected WT and *Robo4*$^{-/-}$ mice to the Cy/G injection schedule of Figure 3A. As expected, WT mice displayed robust increases in BM HSC numbers by day 2 (~20-fold; Figure 3B) and high numbers of PB HSCs starting at day 2 with a further significant increase by day 4 (Figure 3C). *Robo4*$^{-/-}$ HSCs in the BM expanded to similar levels as WT HSCs (Figure 3B), consistent with their normal in vitro proliferation rates and proliferative capacity with in vivo 5-FU treatment (Figure S2). However, contrary to our hypothesis that *Robo4*$^{-/-}$ HSCs would relocate to the blood more efficiently because of weakened niche interactions, we detected significantly fewer *Robo4*$^{-/-}$ HSCs in the PB at day 2 (Figure 3C). This impaired mobilization was specific for HSCs, as MPP numbers in the PB were similar between WT and *Robo4*$^{-/-}$ mice at all time points (Figure 3D).

Sdf1 and Cxcr4 Are Upregulated to Compensate for Loss of Robo4

To determine whether upregulation of other cell surface receptors accounts for the impaired HSC mobilization in *Robo4*$^{-/-}$ mice, we compared the expression of potentially redundant receptors in WT and *Robo4*$^{-/-}$ HSCs. We did not detect compensatory increases in Robo1, Robo2, or Robo3 mRNA levels in *Robo4*$^{-/-}$ HSCs (data not shown), and we failed to detect cell surface Robo1 on either WT or *Robo4*$^{-/-}$ HSCs (Figure S1B and data not shown). Likewise, we detected no differences in the levels of Vcam1, CD31, or Esam1 (Figure S3A). Because Cxcr4 has been suggested to retain HSCs in BM niches by interaction with Sdf1-expressing cells, we assayed the effect of Robo4 deficiency on Cxcr4 expression. Strikingly, we observed a 3-fold increase in Cxcr4 transcript levels in *Robo4*$^{-/-}$ mice (Figure 3E). Transcription did not appear to be regulated by levels of histone H3 trimethylation of lysine 4 (H3K4Me3) and 27 (H3K27Me3) (Figures S3B and S3C). However, elevated Cxcr4 transcript levels were paralleled by increased cell surface levels of Cxcr4 on HSCs, but not on MPP or myeloid progenitor cells (Figure 3F). In addition, we observed an increase in Sdf1 mRNA levels in BM stromal cells in *Robo4*$^{-/-}$ mice (Figure 3G). Interestingly, expression of Slit2 was not affected by loss of Robo4 (Figure 3H). These results demonstrated a specific upregulation of the Sdf1/Cxcr4 axis in *Robo4*$^{-/-}$ BM.

Intriguingly, Cy/G treatment led to decreased Sdf1 expression in BM stromal cells in both WT and *Robo4*$^{-/-}$ mice (Figure 3G). In addition, Cxcr4 cell surface levels increased on BM HSCs, but decreased on HSCs in PB upon Cy/G treatment (Figure 3I). These results suggest that daily G injections eventually overcome Cxcr4-mediated retention of HSC, and that only the highest Cxcr4-expressing HSCs remain in the BM by day 4. The observation that Cy/G treatment affects Cxcr4 levels also support our hypothesis that the elevated levels of Cxcr4 in *Robo4*$^{-/-}$ HSCs accounts for their poor mobilization by day 2 (Figure 3C).

NIH-PA Author Manuscript

NIH-PA Author Manuscript

NIH-PA Author Manuscript

Inhibition of Cxcr4 Restores Cy/G-Induced HSC Mobilization Efficiency in *Robo4*$^{-/-}$ Mice

If upregulation of Cxcr4 acts as a compensatory mechanism to counteract the loss of Robo4, inhibition of Cxcr4-mediated interaction with BM niche components should restore the mobilization efficiency of *Robo4*$^{-/-}$ HSCs. To test this possibility directly, we performed mobilization assays by using Cy/G combined with the Cxcr4 inhibitor AMD3100 according to the injection schedule of Figure 4A. BM and PB analysis of HSCs in WT mice revealed no significant differences between treatment with Cy/G alone or Cy/G plus AMD3100 (Figure 4B). Strikingly, combined Cy/G and AMD3100 treatment of *Robo4*$^{-/-}$ mice resulted in significantly better HSC mobilization than Cy/G alone, restoring *Robo4*$^{-/-}$ HSC levels in the PB to that of WT HSC (Figure 4B). This effect was unique to HSCs, as there was no differential response between WT and *Robo4*$^{-/-}$ MPP under these conditions (Figure 4C). These results support our hypothesis that upregulation of Cxcr4 compensates for loss of Robo4-mediated interactions between HSC and BM niches.

Differential Mobilization of Hematopoietic Stem and Progenitors by AMD3100

We also investigated the effects of AMD3100 alone on HSC mobilization in WT and *Robo4*$^{-/-}$ mice. Although progenitor cell numbers increased robustly in the blood 1 hr after two sequential AMD3100 injections, we found surprisingly few circulating HSCs in WT mice (Figure 4D). These results were consistent with different injection schedules and routes (i.v., s.c.). Thus, MPP and myeloid progenitors were mobilized more efficiently with AMD3100 than were HSCs.

We hypothesized that the relatively low mobilization efficiency with AMD3100 is due to HSC retention in BM niches by non-Cxcr4-mediated, HSC-specific interactions such as Robo4 adhesion. Intriguingly, the efficiency of AMD3100-induced HSC, but not progenitor, mobilization was much greater in *Robo4*$^{-/-}$ mice compared to WT mice (Figure 4E). In vitro colony-forming assays were consistent with these data (Figure S4). This supports the hypothesis that Robo4 acts to retain HSCs in the BM niche in collaboration with Cxcr4, and that Cxcr4 upregulation compensates for Robo4 loss.

HSCs Express Relatively Low Levels of Cxcr4 and Migrate Less Efficiently toward Sdf1

When investigating Cxcr4 expression (Figure 3F), we were surprised to find very low Cxcr4 cell surface levels on WT HSCs. Those results and the differential response of HSCs and progenitors to AMD3100 (Figure 4D) prompted us to investigate the relative importance of Cxcr4 for different BM subpopulations. We first compared Cxcr4 expression levels by qRT-PCR. In agreement with published literature, we found very high levels of Cxcr4 transcripts in B cells (Figure 5A). HSCs also expressed Cxcr4 mRNA, although at lower levels than several other cell types. A very similar pattern was observed when analyzing Cxcr4 cell surface levels by flow cytometry (Figure 5B), revealing that several cell types that are more numerous than HSCs display much higher levels of Cxcr4 (Figure 5C).

We therefore tested the functional consequences of differential Cxcr4 levels by comparing the in vitro migratory response of different populations to Sdf1 (Aiuti et al., 1997). Although we detected robust and reproducible HSC migration toward Sdf1, cell types expressing higher levels of Cxcr4 (e.g., MPP, myeloid progenitors, and B cells) migrated with significantly greater efficiency (Figures 5C and 5D). These results suggest that the Sdf1/Cxcr4 axis affects hematopoietic progenitor cells to a greater extent than HSCs, consistent with the higher mobilization efficiency of progenitors with AMD3100 in vivo (Figures 4B–4D).

Because Robo receptors on brain and endothelial cells are capable of mediating migratory responses to Slit ligands, we hypothesized that Slit2 might attract or repel HSCs. However,

NIH-PA Author Manuscript

NIH-PA Author Manuscript

NIH-PA Author Manuscript

we did not detect HSC migration toward Slit2 (data not shown) under conditions where HSC migration toward Sdf1 is readily detected (Figure 5D). Because Slits can act as repellants (Park et al., 2003; Seth et al., 2005), we also tested whether Slit2 inhibited HSC migration toward Sdf1. Neither preincubation of HSC with Slit2 nor addition of Slit2 to Sdf1-containing bottom wells had an effect on Sdf1-induced HSC migration (Figure S5A); likewise, migration of $CD4^+$ T cells was not affected (Figure S5B). We confirmed that Slit2 was biologically active by demonstrating inhibition of HL60 cell migration toward fMLP (Figure S5C). Thus, Robo4 expression on HSCs does not translate to detectable migratory responses in vitro.

Robo4 and Cxcr4 Cooperate to Localize HSCs to the BM upon Transplantation

The upregulation of Cxcr4 upon loss of Robo4 (Figures 3E and 3F) and the increased mobilization efficiency with AMD3100 in *Robo4*$^{-/-}$ mice (Figure 4E) prompted us to investigate the role of Cxcr4 and Robo4 on HSC localization to the BM upon transplantation. We first tested whether preincubation with AMD3100 was capable of inhibiting HSC migration toward Sdf1 in transwell migration assays. Indeed, we detected a dose-dependent decrease in migration of both WT and *Robo4*$^{-/-}$ HSCs, with complete inhibition at 12.5 μM of AMD3100 (Figure 6A; Figure S6).

We then transplanted untreated and AMD3100-treated HSCs from WT and *Robo4*$^{-/-}$ mice into lethally irradiated recipients. Three hours postinjection, BM, spleen, and PB were analyzed for numbers of donor cells. In contrast to in vitro migration, where AMD3100 completely abolished migration of HSCs toward Sdf1 (Figure 6A), AMD3100 was not expected to completely inhibit homing in vivo because *Cxcr4*$^{-/-}$ HSCs are capable of BM engraftment (Nie et al., 2008; Sugiyama et al., 2006). Consistent with this observation, AMD3100 preincubation of WT cells resulted in a ~2-fold reduction in donor cells localizing to the BM (Figure 6B). Loss of Robo4 led to a comparable decrease in transplanted cells in the BM (Figure 6B), a notable result because this decrease occurred despite the elevated levels of Cxcr4 on *Robo4*$^{-/-}$ HSCs (Figure 3F). Strikingly, treatment of Robo4-deficient cells with AMD3100 resulted in a further decrease in BM localization (Figure 6B), demonstrating that both Robo4 and Cxcr4 function to localize HSCs to the BM upon transplantation. Consistent with the decreased number of transplanted cells in the BM for each condition, a reciprocal increase of donor cells was detected in the bloodstream (Figure 6C). Interestingly, there were no differences in localization to the spleen (Figure 6D), supporting the BM-specific effects observed with *Robo4*$^{-/-}$ HSCs in steady state, CFU-S, and multilineage reconstitution assays (Figure 2; Figure S2). These data demonstrate that Robo4 and Cxcr4, individually and together, regulate HSC localization to the BM.

Discussion

Robo4 Regulates HSC Interactions with BM Niches

We have identified Robo4 as a critical regulator of HSC localization to the BM. Robo4 expression was very low in fetal HSCs residing in the liver, but increased during development concurrent with the establishment of BM hematopoiesis (Figure 1C). Thus, Robo4 is very selectively expressed by adult BM HSCs and downregulation occurs not only during normal differentiation, but also upon HSC mobilization and in leukemogenesis (Figures 1A and 1B). Intriguingly, these processes all involve alterations in cell location, concomitant with a surge in proliferation. Although we have not yet assessed the functional role of Robo4 in leukemic transformation, its downregulation in L-HSCs is consistent with the proposed tumor suppressor functions of Robo receptors (Dallol et al., 2002; Legg et al., 2008; Marlow et al., 2008). Thus, downregulation of Robo4 may be a prerequisite for HSC exit out of BM niches regulating HSC function. Because very few BM cells are Robo4

NIH-PA Author Manuscript

NIH-PA Author Manuscript

NIH-PA Author Manuscript

positive, our data suggest that Robo4 is an excellent HSC-specific marker. It will be interesting to investigate the utility of Robo4, alone and in combination with other highly specific HSC markers such as Esam1 (Ooi et al., 2009), in simplified HSC purification protocols.

Consistent with its HSC-specific expression, Robo4 deletion led to perturbations in HSC localization during steady-state (Figure 2A), in short-term homing (Figure 6) and long-term reconstitution assays (Figures 2C and 2F), and upon mobilization with both Cy/G and AMD3100 (Figures 3 and 4). These effects were specific for BM localization, as spleen readouts and in vitro HSC properties were not affected by Robo4 loss (Figures 2E and 6D; Figure S2). Decreased *Robo4*$^{-/-}$ HSC frequencies in BM at steady-state indicates that Robo4 stabilizes interactions between HSC and BM niche components. Such a function is consistent with the poor BM localization of *Robo4*$^{-/-}$ HSCs in short-term homing assays and dramatically impaired long-term engraftment. Importantly, the *Robo4*$^{-/-}$ HSCs that did engraft had normal differentiation capacity (Figure 2D). Robo4 function therefore appears restricted to regulating HSC interactions with the BM niche and does not appear to affect cell fate choice. Furthermore, *Robo4*$^{-/-}$ HSCs were more efficiently mobilized with AMD3100 than were WT HSCs (Figure 4E), indicating that Robo4 acts to retain HSCs in BM niches. In contrast to the increased relocation to the blood with AMD3100, Cy/G-induced HSC mobilization was impaired in *Robo4*$^{-/-}$ mice (Figure 3C). Investigation of the underlying molecular mechanisms revealed that Cxcr4 was upregulated in *Robo4*$^{-/-}$ HSCs (Figures 3E and 3F), suggesting that Cxcr4 can compensate for loss of Robo4. Importantly, addition of AMD3100 to the Cy/G regimen restored the mobilization efficiency to WT levels (Figure 4B). This demonstrates that Cxcr4 and Robo4 act together to retain HSCs in the BM. Developmental upregulation of Robo4 and our finding that Robo4 tethers HSCs specifically to BM niches provide a tantalizing explanation for how HSCs gain Cxcr4 independence once seeded in the BM (Sugiyama et al., 2006; Nie et al., 2008).

Slit2 Does Not Affect HSC Function In Vitro

The role of Slits in Robo4 function has been debated, because high-affinity, direct binding of Slit2 protein to Robo4 protein is not detected (Suchting et al., 2005). However, Robo4 expression endows endothelial cells with migratory responses to Slits (Kaur et al., 2006; Park et al., 2003), and Slit2-mediated effects in the vasculature and mammary gland are Robo4 dependent (Jones et al., 2008; London et al., 2010; Marlow et al., 2010). These observations have led to the concept that a coreceptor enhances the affinity of Slit2 for Robo4. Proposed coreceptors include Robo1 (Sheldon et al., 2009) and syndecans (Hu, 2001; Johnson et al., 2004; Steigemann et al., 2004). Because Robo1 is not expressed by HSCs (Figure S1B), syndecans are more likely coreceptor candidates in HSCs. Indeed, we have previously reported differential regulation of syndecan family members between HSCs and progenitor cells (Forsberg et al., 2005). To our knowledge, the functional consequences of this differential expression have not been investigated.

The lack of Slit2 effects on HSC proliferation and migration in vitro does not preclude an important role for Slit2 on HSC function in vivo. Indeed, if Robo4 acts to tether HSCs to BM niches, Slits would be expected to have little impact in solution. Instead, lack of Slit2 effects in vitro supports a role for Slit/Robo signaling in niche-dependent HSC function. Upregulation of Slit2 during hematopoietic stress (Shibata et al., 2009) argues for a physiologically important role of Slit2 in HSC function. The relative importance of this role may be amplified in stress situations, analogous to what has been observed upon challenges to vascular integrity (Jones et al., 2008; London et al., 2010; Marlow et al., 2010).

NIH-PA Author Manuscript

NIH-PA Author Manuscript

NIH-PA Author Manuscript

Differential Efficacy of Cxcr4 Manipulation on Hematopoietic Stem and Progenitor Cells

Cxcr4 is a well-established regulator of HSC localization to the BM. Surprisingly, however, we found that HSCs express relatively low levels of Cxcr4, both at the transcript and cell surface protein levels. These results contrast those by Sugiyama and colleagues, who reported higher Cxcr4 mRNA levels in HSCs compared to MPP (Sugiyama et al., 2006), but are consistent with a recent report assaying Cxcr4 expression and hematopoietic cell migration (Sasaki et al., 2009). Importantly, we showed that differential Cxcr4 expression had functional consequences, as AMD3100-induced mobilization (Figure 4D) and migration efficiency toward Sdf1 (Figure 5D) correlated with Cxcr4 expression levels (Figure 5). Our findings have important implications for understanding the molecular mechanisms of HSC localization next to Sdf1-expressing cells (Sugiyama et al., 2006). Several cell types, far more numerous than HSCs, express higher levels of Cxcr4 (Figure 5) and consequently respond better to Sdf1 and AMD3100 (Figures 4D and 5D). This includes myeloid progenitors, B, and T cells. Therefore, molecules other than Cxcr4 must specify location of HSCs to limited niche space. Indeed, we show that Robo4 collaborates with Cxcr4 to provide highly HSC-specific localization cues.

Because the molecular mechanisms mobilizing mouse and human HSCs are remarkably similar, Robo4 cooperation with Cxcr4 have potentially important clinical implications. A bolus injection of AMD3100 alone does not yield sufficient numbers of HSCs for an adult transplant. Therefore, alternative injection protocols and combinatorial use with other mobilizing agents have been explored, including continuous AMD3100 infusion, and AMD3100 combined with G-CSF and integrin α4 inhibitors (Bonig et al., 2009; Flomenberg et al., 2005; Liles et al., 2003). A mobilizing agent specifically targeting HSCs, such as an inhibitor of Robo4-mediated adhesion, may significantly boost HSC yield.

Robo4 and Cxcr4 Employ Distinct Molecular Mechanisms to Localize HSCs to the BM

The HSC phenotype upon Robo4 loss is similar to that of conditional deletion or AMD3100-mediated inhibition of Cxcr4. For example, deletion of Robo4 and AMD3100 treatment resulted in similar decreases in HSC localization to the BM 3 hr postinjection (Figure 6B), and at steady state, HSC BM frequencies were decreased upon either Robo4 (Figure 2A) or Cxcr4 (Sugiyama et al., 2006) deletion. In addition, both *Robo4*$^{-/-}$ and *Cxcr4*$^{-/-}$ HSCs display lower long-term engraftment but retained lineage multipotency (Figures 2C and 2D; Nie et al., 2008; Sugiyama et al., 2006). However, important differences distinguish the mechanisms of receptor function. Cxcr4 expression endows HSCs with an active migratory response toward Sdf1, but we were unable to detect such effects with Slit2. Additionally, Cxcr4 is expressed by many hematopoietic and nonhematopoietic cell types, whereas Robo4 expression is highly selective for HSCs. Indeed, our functional data demonstrate highly HSC-specific functions for Robo4.

In a simplified model, chemoattractants, including Sdf1, guide HSCs to the BM (Figure 7). Once in the vicinity of HSC-supportive niches, Cxcr4 and Robo4 together promote HSC retention in the niche and stable engraftment. The highly HSC-restricted Robo4 expression probably endows HSCs with a competitive advantage to limited BM niche space compared to cells expressing higher levels of Cxcr4, but not Robo4. Inhibition or loss of Cxcr4 results in fewer HSCs actively migrating toward niches. Loss of Robo4, on the other hand, probably results in equal, or because of Cxcr4 upregulation maybe even greater, numbers of HSCs localizing close to niches. However, BM localization is transient in the absence of Robo4 because fewer HSCs engage in stable niche interactions. In both cases, decreased long-term engraftment is observed. Because of these dual cooperative adhesive cues, both Robo4- and Cxcr4-mediated interactions with the niche have to be inhibited for efficient HSC

NIH-PA Author Manuscript

NIH-PA Author Manuscript

NIH-PA Author Manuscript

mobilization to the blood; thus, AMD3100-induced HSC mobilization is more efficient in Robo4-deficient mice.

Receptor Redundancy in the Control of HSC Function

Upregulation of Cxcr4 seems to partially compensate for Robo4 loss and attenuate the phenotype of *Robo4*$^{-/-}$ mice. This is supported by the inefficient HSC mobilization with Cy/G in *Robo4*$^{-/-}$ mice (Figure 3C) and additive effects in BM homing experiments (Figure 6B). Likewise, engraftment of *Cxcr4*$^{-/-}$ HSCs is likely possible due to functional redundancy with Robo4 and other adhesion receptors expressed by HSCs. Although we did not detect upregulation of Vcam1, Esam1, or CD31 upon Robo4 deletion, these receptors are highly expressed by HSCs (Figure S3A), and probably contribute to HSC localization (Kikuta et al., 2000; Ooi et al., 2009; Ross et al., 2008). In the vasculature, Robo4 intersects with pathways regulated by VE-cadherin and VEGF receptors. Because VEGF signaling and the sinusoidal endothelium affects hematopoietic reconstitution (Hooper et al., 2009), Robo4 may also affect hematopoiesis by its expression in endothelial cells. We recently reported increased defects in angiogenesis under pathological conditions in *Robo4*$^{-/-}$ mice (Jones et al., 2008) and we also found that Robo4 controls blood vessel growth during mammary gland development (Marlow et al., 2010). These reports demonstrated that Robo4 is dispensable under homeostatic conditions, but critically important during tissue perturbation and remodeling. Mechanistically, it is intriguing that the Sdf1/Cxcr4 axis is upregulated in *Robo1*$^{-/-}$ mammary glands (Marlow et al., 2008). These results point to conservation of molecular mechanisms across tissues and between different Robo receptors.

Several molecules have been implicated in HSC homing and engraftment, but the relationship between these factors and how they work together to specify HSC location is unclear. We recently proposed a “niche code hypothesis,” where HSC location is specified by a combination of factors, much like the histone code hypothesis dictates transcriptional outcome (Forsberg and Smith-Berdan, 2009). This model takes into account the contribution of multiple receptors in regulating HSC location and function. Such receptor redundancy would also allow HSCs to respond to multiple types of cues to stimulate production of the appropriate cell type. We have begun to dissect this complex regulation by establishing a functional relationship between Robo4 and Cxcr4 in controlling HSC location. A sophisticated understanding of the molecular cues from the endogenous niche milieu that support HSC self-renewal will be necessary to overcome our frustrating inability to expand and generate transplantable HSCs ex vivo.

Therapeutic Potential of Manipulating Robo4 Function

The responsiveness of Robo receptors to soluble ligands renders them optimal targets for manipulation by natural or synthetic agonists and antagonists. A relevant precedence is provided by the clinical utility of Cxcr4 antagonists in hematopoietic cell mobilization. However, Cxcr4 is expressed by many different cell types, including the brain, leading to significant effects on non-HSC populations, and genetic *Cxcr4* deletion is embryonic lethal. In contrast, *Robo4*$^{-/-}$ mice are viable with mild phenotype, and Robo4 expression is restricted to HSCs and endothelial cells. Thus, pharmacologic manipulation of Robo4 function will probably be safe and highly specific. Once potent modulators of Robo4 function have been identified, Robo4 is a potentially valuable clinical target to improve the success of HSC transplantation therapy.

NIH-PA Author Manuscript

NIH-PA Author Manuscript

NIH-PA Author Manuscript

Experimental Procedures

Mice

Mice were maintained by the UCSC animal facility according to approved protocols. *Robo4*$^{-/-}$ mice were described previously (Jones et al., 2008; London et al., 2010; Marlow et al., 2010). WT mice were generated from het/het breeding of the *Robo4*$^{-/-}$ mice or purchased C57Bl6 mice from JAX (Bar Harbor, Maine). Radiation was delivered as a split dose administered 3 hr apart with a Faxitron CP-160 X-ray instrument (Lincolnshire, IL).

Competitive Reconstitution Assays

HSC were isolated from *Robo4*$^{-/-}$ (Ly5.1) or WT (Ly5.1/5.2) donors by two rounds of FACS and administered i.v. with whole bone marrow helper cells (3e5 cells) from Ly5.2 congenic hosts. Recipient mice were bled at 3, 6, 9, 12, and 16 weeks posttransplant via the tail vein and peripheral blood was analyzed for donor chimerism by means of antibodies to the Ly5.1 (Alexa488) and Ly5.2 (Alexa680) alleles and the lineage markers B220 (APC-Cy7), CD3 (PE), Mac1 (PECy7), Ter119 (PECy5), and Gr1 (Pacific Blue) (eBioscience, Biolegend, or BD Biosciences). Statistically significant differences for all comparisons were calculated with two-tailed t tests, unless stated otherwise.

qRT-PCR

Quantitative RT-PCR was performed as described previously (Forsberg et al., 2005, 2006), except reactions were conducted on a Corbett cycler with the Quantace SensiMixPlus SYBR. Expression of β-actin was used to normalize cDNA amounts between samples.

Modified Boyden Migration Assays

BM cells (lineage depleted by magnetic selection, when appropriate), were preincubated at 37°C for 1 hr, then placed in the upper chamber of a transwell insert (5 μm pore size). Bottom and/or top wells contained Sdf1 (100 ng/ml) and/or Slit2, as indicated. Cells were allowed to migrate for 2 hr at 37°C before harvesting and analysis by flow cytometry.

Cy/G and AMD3100 Mobilization

Mice were mobilized with cytoxan and G-CSF (Cy/G) as previously described (Morrison et al., 1997). In brief, mice were injected i.p. with 200 mg/kg of Cytoxan in HBSS (Sigma-Aldrich) on day –1, followed by two or four sequential daily s.c. injections of 200 mg/kg rhG-CSF (Humanzyme, Chicago, IL). Tissues were analyzed on day 2 or 4, as indicated (Figures 3A and 4A). A cohort from each group was injected i.v. with 5 mg/kg of AMD3100 1 hr prior to sacrifice. For AMD3100 alone, mice were treated with two serial AMD3100 (5 mg/kg) i.v. injections 1 hr apart. Peripheral blood, spleen, and bone marrow were isolated 1 hr later and processed for cell counts and flow cytometry analysis to determine the numbers and frequencies of each cell population.

BM Homing Assays

BM cells were labeled with CFSE labeling dye (Invitrogen) for 5 min at rt, followed by antibody labeling and isolation of cKit^{+}/Lin^{neg}/Sca1^{+}/CFSE^{hi} cells by two rounds of FACS. Sorted cells were split in two equal parts and incubated with or without AMD3100 (12.5 μM) on ice for 30 min. Cells were washed, pelleted by centrifugation, and resuspended in HBSS at 400,000 cells/ml. Hosts, lethally irradiated 24 hr prior to transplantation, were injected i.v. with 40,000 cells in 100 μl. Three hours posttransplant, tissues were harvested from individual mice and analyzed for CFSE-labeled cells by flow cytometry.

NIH-PA Author Manuscript

NIH-PA Author Manuscript

NIH-PA Author Manuscript

Supplementary Material

Refer to Web version on PubMed Central for supplementary material.

Acknowledgments

We thank Dr. Andrew Leavitt for generously providing reagents. This work was funded by University of California Santa Cruz start-up funds (E.C.F.); California Institute for Regenerative Medicine (CIRM) Stem Cell Training Program Awards (A.N., F.U., and J.C.); a UCSC Minority Access to Research Careers Fellowship (D.H.); a postdoctoral fellowship from the Government of Navarra, Spain (J.C.); and University of California, Merced start-up funds (M.E.G.-O.). D.L. is supported by the DOD, AAF, JDRF, and NIH. L.H. was partially funded by NIH (RO1 CA-128902). E.C.F. is the recipient of a CIRM New Faculty Award. University of Utah has licensed intellectual property surrounding the Robo4 pathway to Navigen. Both the University of Utah and D.Y.L. have equity in Navigen.

References

Aiuti A, Webb IJ, Bleul C, Springer T, Gutierrez-Ramos JC. The chemokine SDF-1 is a chemoattractant for human CD34+ hematopoietic progenitor cells and provides a new mechanism to explain the mobilization of CD34+ progenitors to peripheral blood. J Exp Med. 1997; 185:111–120. [PubMed: 8996247]

Bonig H, Chudziak D, Priestley G, Papayannopoulou T. Insights into the biology of mobilized hematopoietic stem/progenitor cells through innovative treatment schedules of the CXCR4 antagonist AMD3100. Exp Hematol. 2009; 37:402–415. e1. [PubMed: 19157683]

Broxmeyer HE, Orschell CM, Clapp DW, Hangoc G, Cooper S, Plett PA, Liles WC, Li X, Graham-Evans B, Campbell TB, et al. Rapid mobilization of murine and human hematopoietic stem and progenitor cells with AMD3100, a CXCR4 antagonist. J Exp Med. 2005; 201:1307–1318. [PubMed: 15837815]

Dallol A, Forgacs E, Martinez A, Sekido Y, Walker R, Kishida T, Rabbitts P, Maher ER, Minna JD, Latif F. Tumour specific promoter region methylation of the human homologue of the *Drosophila* Roundabout gene DUTT1 (ROBO1) in human cancers. Oncogene. 2002; 21:3020–3028. [PubMed: 12082532]

Flomenberg N, DiPersio J, Calandra G. Role of CXCR4 chemokine receptor blockade using AMD3100 for mobilization of autologous hematopoietic progenitor cells. Acta Haematol. 2005; 114:198–205. [PubMed: 16269859]

Forsberg EC, Smith-Berdan S. Parsing the niche code: The molecular mechanisms governing hematopoietic stem cell adhesion and differentiation. Haematologica. 2009; 94:1477–1481. [PubMed: 19880773]

Forsberg EC, Prohaska SS, Katzman S, Heffner GC, Stuart JM, Weissman IL. Differential expression of novel potential regulators in hematopoietic stem cells. PLoS Genet. 2005; 1:e28. [PubMed: 16151515]

Forsberg EC, Serwold T, Kogan S, Weissman IL, Passegué E. New evidence supporting megakaryocyte-erythrocyte potential of flk2/flt3+ multipotent hematopoietic progenitors. Cell. 2006; 126:415–426. [PubMed: 16873070]

Forsberg EC, Passegué E, Prohaska SS, Wagers AJ, Koeva M, Stuart JM, Weissman IL. Molecular signatures of quiescent, mobilized and leukemia-initiating hematopoietic stem cells. PLoS ONE. 2010; 5:e8785. [PubMed: 20098702]

Hooper AT, Butler JM, Nolan DJ, Kranz A, Iida K, Kobayashi M, Kopp HG, Shido K, Petit I, Yanger K, et al. Engraftment and reconstitution of hematopoiesis is dependent on VEGFR2-mediated regeneration of sinusoidal endothelial cells. Cell Stem Cell. 2009; 4:263–274. [PubMed: 19265665]

Hu H. Cell-surface heparan sulfate is involved in the repulsive guidance activities of Slit2 protein. Nat Neurosci. 2001; 4:695–701. [PubMed: 11426225]

Huminiecki L, Gorn M, Suchting S, Poulsom R, Bicknell R. Magic roundabout is a new member of the roundabout receptor family that is endothelial specific and expressed at sites of active angiogenesis. Genomics. 2002; 79:547–552. [PubMed: 11944987]

NIH-PA Author Manuscript

NIH-PA Author Manuscript

NIH-PA Author Manuscript

Johnson KG, Ghose A, Epstein E, Lincecum J, O'Connor MB, Van Vactor D. Axonal heparan sulfate proteoglycans regulate the distribution and efficiency of the repellent slit during midline axon guidance. Curr Biol. 2004; 14:499–504. [PubMed: 15043815]

Jones CA, London NR, Chen H, Park KW, Sauvaget D, Stockton RA, Wythe JD, Suh W, Larrieu-Lahargue F, Mukouyama YS, et al. Robo4 stabilizes the vascular network by inhibiting pathologic angiogenesis and endothelial hyperpermeability. Nat Med. 2008; 14:448–453. [PubMed: 18345009]

Kaur S, Castellone MD, Bedell VM, Konar M, Gutkind JS, Ramchandran R. Robo4 signaling in endothelial cells implies attraction guidance mechanisms. J Biol Chem. 2006; 281:11347–11356. [PubMed: 16481322]

Kikuta T, Shimazaki C, Ashihara E, Sudo Y, Hirai H, Sumikuma T, Yamagata N, Inaba T, Fujita N, Kina T, Nakagawa M. Mobilization of hematopoietic primitive and committed progenitor cells into blood in mice by anti-vascular adhesion molecule-1 antibody alone or in combination with granulocyte colony-stimulating factor. Exp Hematol. 2000; 28:311–317. [PubMed: 10720696]

Lapidot T. Mechanism of human stem cell migration and repopulation of NOD/SCID and B2mnull NOD/SCID mice. The role of SDF-1/CXCR4 interactions. Ann N Y Acad Sci. 2001; 938:83–95. [PubMed: 11458529]

Legg JA, Herbert JM, Clissold P, Bicknell R. Slits and Roundabouts in cancer, tumour angiogenesis and endothelial cell migration. Angiogenesis. 2008; 11:13–21. [PubMed: 18264786]

Liles WC, Broxmeyer HE, Rodger E, Wood B, Hübel K, Cooper S, Hangoc G, Bridger GJ, Henson GW, Calandra G, Dale DC. Mobilization of hematopoietic progenitor cells in healthy volunteers by AMD3100, a CXCR4 antagonist. Blood. 2003; 102:2728–2730. [PubMed: 12855591]

London NR, Zhu W, Bozza FA, Smith MC, Greif DM, Sorensen LK, Chen L, Kaminoh Y, Chan AC, Passi SF, et al. Targeting Robo4-dependent Slit signaling to survive the cytokine storm in sepsis and influenza. Sci Transl Med. 2010; 2:ra19.

Marlow R, Strickland P, Lee JS, Wu X, Pebenito M, Binnewies M, Le EK, Moran A, Macias H, Cardiff RD, et al. SLITs suppress tumor growth in vivo by silencing Sdf1/Cxcr4 within breast epithelium. Cancer Res. 2008; 68:7819–7827. [PubMed: 18829537]

Marlow R, Binnewies M, Sorensen LK, Monica SD, Strickland P, Forsberg EC, Li DY, Hinck L. Vascular Robo4 restricts proangiogenic VEGF signaling in breast. Proc Natl Acad Sci USA. 2010; 107:10520–10525. [PubMed: 20498081]

Morrison SJ, Wright DE, Weissman IL. Cyclophosphamide/granulocyte colony-stimulating factor induces hematopoietic stem cells to proliferate prior to mobilization. Proc Natl Acad Sci USA. 1997; 94:1908–1913. [PubMed: 9050878]

Nagasawa T, Hirota S, Tachibana K, Takakura N, Nishikawa S, Kitamura Y, Yoshida N, Kikutani H, Kishimoto T. Defects of B-cell lymphopoiesis and bone-marrow myelopoiesis in mice lacking the CXC chemokine PBSF/SDF-1. Nature. 1996; 382:635–638. [PubMed: 8757135]

Nie Y, Han YC, Zou YR. CXCR4 is required for the quiescence of primitive hematopoietic cells. J Exp Med. 2008; 205:777–783. [PubMed: 18378795]

Ooi AG, Karsunky H, Majeti R, Butz S, Vestweber D, Ishida T, Quertermous T, Weissman IL, Forsberg EC. The adhesion molecule esam1 is a novel hematopoietic stem cell marker. Stem Cells. 2009; 27:653–661. [PubMed: 19074415]

Park KW, Morrison CM, Sorensen LK, Jones CA, Rao Y, Chien CB, Wu JY, Urness LD, Li DY. Robo4 is a vascular-specific receptor that inhibits endothelial migration. Dev Biol. 2003; 261:251–267. [PubMed: 12941633]

Passegué E, Wagner EF, Weissman IL. JunB deficiency leads to a myeloproliferative disorder arising from hematopoietic stem cells. Cell. 2004; 119:431–443. [PubMed: 15507213]

Passegué E, Wagers AJ, Giuriato S, Anderson WC, Weissman IL. Global analysis of proliferation and cell cycle gene expression in the regulation of hematopoietic stem and progenitor cell fates. J Exp Med. 2005; 202:1599–1611. [PubMed: 16330818]

Peled A, Petit I, Kollet O, Magid M, Ponomaryov T, Byk T, Nagler A, Ben-Hur H, Many A, Shultz L, et al. Dependence of human stem cell engraftment and repopulation of NOD/SCID mice on CXCR4. Science. 1999; 283:845–848. [PubMed: 9933168]

NIH-PA Author Manuscript

NIH-PA Author Manuscript

NIH-PA Author Manuscript

Prasad A, Qamri Z, Wu J, Ganju RK. Slit-2/Robo-1 modulates the CXCL12/CXCR4-induced chemotaxis of T cells. J Leukoc Biol. 2007; 82:465–476. [PubMed: 17565045]

Ross EA, Freeman S, Zhao Y, Dhanjal TS, Ross EJ, Lax S, Ahmed Z, Hou TZ, Kalia N, Egginton S, et al. A novel role for PECAM-1 (CD31) in regulating haematopoietic progenitor cell compartmentalization between the peripheral blood and bone marrow. PLoS ONE. 2008; 3:e2338. [PubMed: 18523558]

Sasaki Y, Matsuoka Y, Hase M, Toyohara T, Murakami M, Takahashi M, Nakatsuka R, Uemura Y, Sonoda Y. Marginal expression of CXCR4 on c-kit(+)Sca-1 (+)Lineage (-) hematopoietic stem/progenitor cells. Int J Hematol. 2009; 90:553–560. [PubMed: 19937482]

Seth P, Lin Y, Hanai J, Shivalingappa V, Duyao MP, Sukhatme VP. Magic roundabout, a tumor endothelial marker: Expression and signaling. Biochem Biophys Res Commun. 2005; 332:533–541. [PubMed: 15894287]

Sheldon H, Andre M, Legg JA, Heal P, Herbert JM, Sainson R, Sharma AS, Kitajewski JK, Heath VL, Bicknell R. Active involvement of Robo1 and Robo4 in filopodia formation and endothelial cell motility mediated via WASP and other actin nucleation-promoting factors. FASEB J. 2009; 23:513–522. [PubMed: 18948384]

Shibata F, Goto-Koshino Y, Morikawa Y, Komori T, Ito M, Fukuchi Y, Houchins JP, Tsang M, Li DY, Kitamura T, Nakajima H. Roundabout 4 is expressed on hematopoietic stem cells and potentially involved in the niche-mediated regulation of the side population phenotype. Stem Cells. 2009; 27:183–190. [PubMed: 18927479]

Steigemann P, Molitor A, Fellert S, Jäckle H, Vorbrüggen G. Heparan sulfate proteoglycan syndecan promotes axonal and myotube guidance by slit/robo signaling. Curr Biol. 2004; 14:225–230. [PubMed: 14761655]

Suchting S, Heal P, Tahtis K, Stewart LM, Bicknell R. Soluble Robo4 receptor inhibits in vivo angiogenesis and endothelial cell migration. FASEB J. 2005; 19:121–123. [PubMed: 15486058]

Sugiyama T, Kohara H, Noda M, Nagasawa T. Maintenance of the hematopoietic stem cell pool by CXCL12-CXCR4 chemokine signaling in bone marrow stromal cell niches. Immunity. 2006; 25:977–988. [PubMed: 17174120]

Watt SM, Forde SP. The central role of the chemokine receptor, CXCR4, in haemopoietic stem cell transplantation: Will CXCR4 antagonists contribute to the treatment of blood disorders? Vox Sang. 2008; 94:18–32. [PubMed: 18042197]

Wright DE, Cheshier SH, Wagers AJ, Randall TD, Christensen JL, Weissman IL. Cyclophosphamide/granulocyte colony-stimulating factor causes selective mobilization of bone marrow hematopoietic stem cells into the blood after M phase of the cell cycle. Blood. 2001; 97:2278–2285. [PubMed: 11290588]

Wright DE, Bowman EP, Wagers AJ, Butcher EC, Weissman IL. Hematopoietic stem cells are uniquely selective in their migratory response to chemokines. J Exp Med. 2002; 195:1145–1154. [PubMed: 11994419]

Wu JY, Feng L, Park HT, Havlioglu N, Wen L, Tang H, Bacon KB, Jiang Zh Zhang Xc, Rao Y. The neuronal repellent Slit inhibits leukocyte chemotaxis induced by chemotactic factors. Nature. 2001; 410:948–952. [PubMed: 11309622]

Zou YR, Kottmann AH, Kuroda M, Taniuchi I, Littman DR. Function of the chemokine receptor CXCR4 in haematopoiesis and in cerebellar development. Nature. 1998; 393:595–599. [PubMed: 9634238]

NIH-PA Author Manuscript
NIH-PA Author Manuscript
NIH-PA Author Manuscript

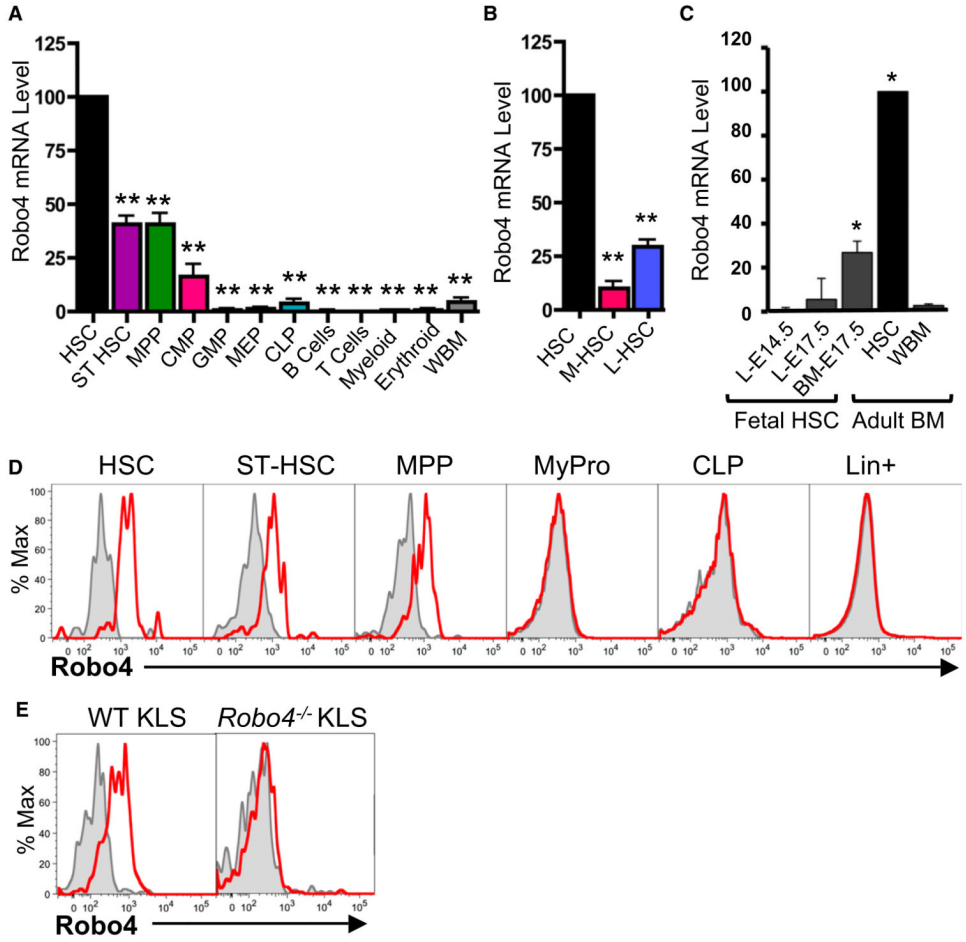

Figure 1. Robo4 Is Selectively Expressed by BM-Localized HSCs

(A) Relative levels of Robo4 transcripts in purified BM populations by qRT-PCR compared to HSCs. Data shown are from four independent experiments with qPCR reactions performed in triplicate.

(B) Relative Robo4 mRNA levels by qRT-PCR in WT HSCs, mobilized HSCs (M-HSCs), and leukemic HSCs (L-HSCs).

(C) Quantitative RT-PCR revealed that Robo4 expression increases as HSCs (defined as ckit^{+}Lin^{-}Sca1^{+} cells) transition from fetal liver (L) to BM during development.

(D) Cell surface Robo4 expression on BM subpopulations from WT mice, demonstrating highly selective Robo4 expression on HSCs.

(E) Flow cytometry plots of ckit^{+}Lin^{-}Sca1^{+} BM cells from WT and *Robo4*$^{-/-}$ mice demonstrating the specificity of the antibody for Robo4.

BM, bone marrow. Error bars represent SEM. *p < 0.005; **p < 0.0001. See also Figure S1.

NIH-PA Author Manuscript

NIH-PA Author Manuscript

NIH-PA Author Manuscript

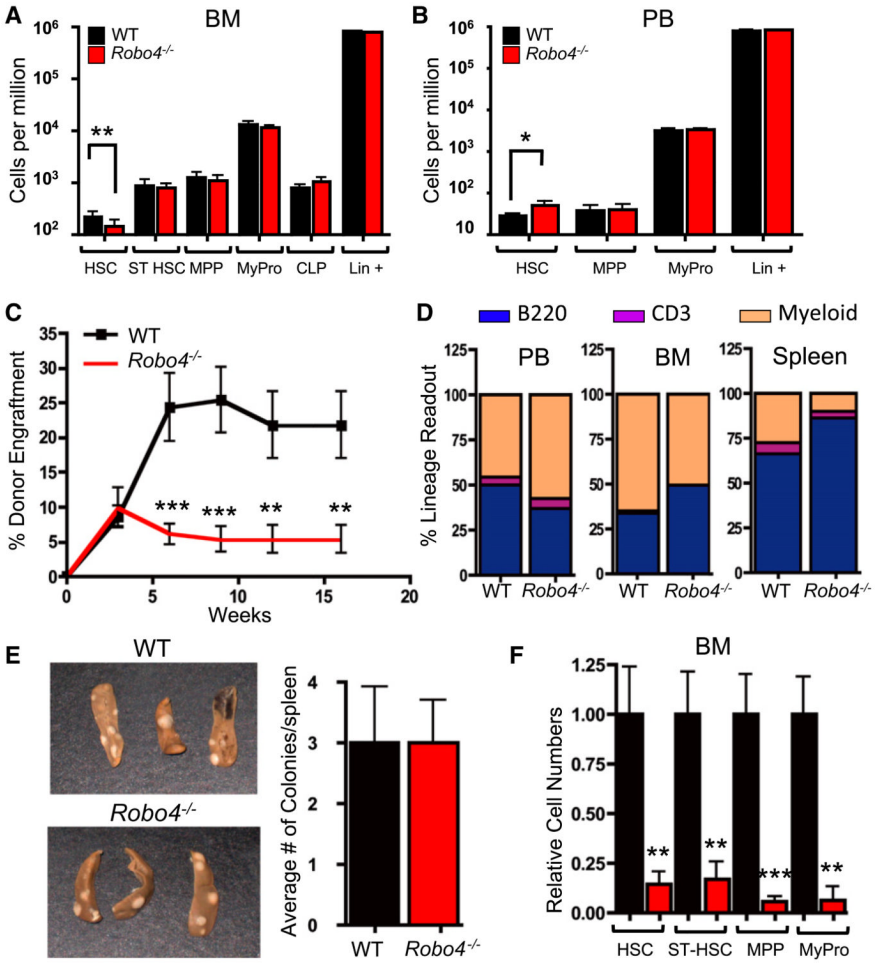

Figure 2. Robo4$^{-/-}$ HSCs Displayed Impaired BM Localization at Steady-State and upon Transplantation

(A and B) HSC frequencies were significantly lower in the BM (A) and higher in PB (B) in *Robo4*$^{-/-}$ mice compared to WT mice. Other cell types were not affected by Robo4 loss.

(C) *Robo4*$^{-/-}$ HSCs had drastically impaired long-term reconstitution potential upon transplantation compared to WT HSCs. Total donor-derived cells in PB at the indicated time points after competitive reconstitution with 100 WT and *Robo4*$^{-/-}$ HSCs are shown.

(D) Relative lineage readout was not affected by Robo4 deficiency. The ratios of mature B, T, and myeloid cells in PB, BM, and spleen >16 weeks after competitive transplantation of 100 WT and *Robo4*$^{-/-}$ HSCs are shown.

(E) *Robo4*$^{-/-}$ HSCs gave rise to in vivo spleen colonies with normal frequencies. Lethally irradiated mice were transplanted with either 100 *Robo4*$^{-/-}$ or WT HSCs. Twelve days after transplantation, spleens were harvested for CFU-S analysis.

(F) The number of *Robo4*$^{-/-}$ HSCs and progenitor cells in the BM of transplanted mice was significantly lower than WT cells at >16 weeks posttransplantation.

All data are from at least three independent experiments with at least three mice per group per experiment ($n \geq 9$). Error bars represent SEM. **$p < 0.004$; ***$p < 0.0006$. See also Figure S2.

NIH-PA Author Manuscript
NIH-PA Author Manuscript
NIH-PA Author Manuscript

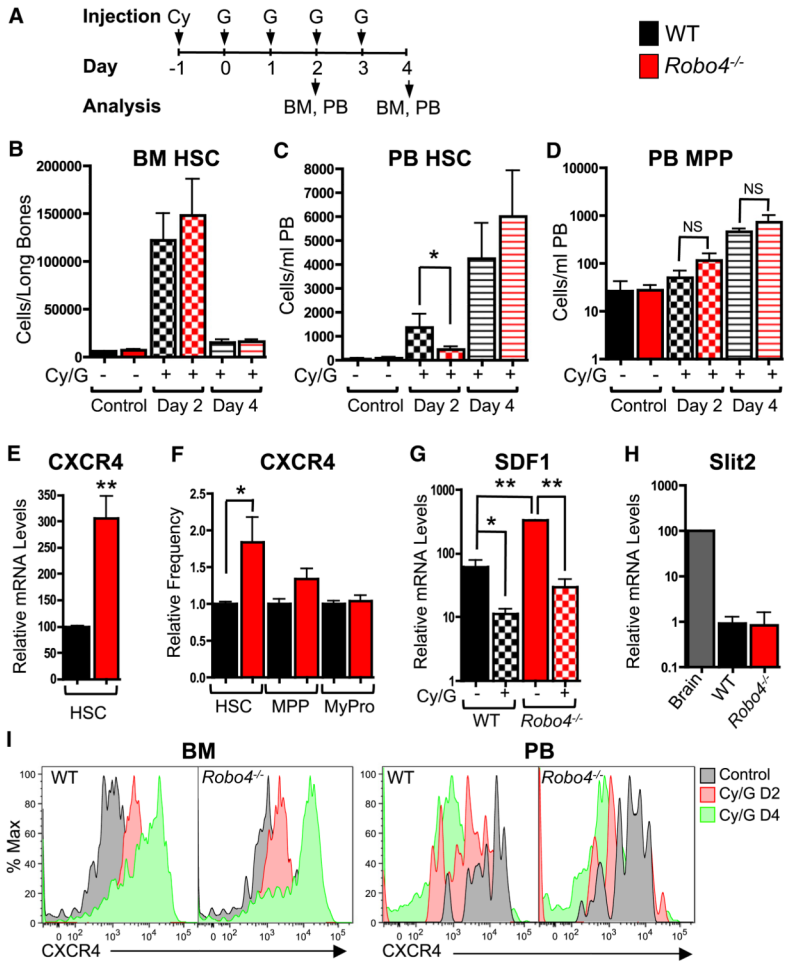

Figure 3. Robo4$^{-/-}$ HSCs Mobilized Less Efficiently with Cy/G Treatment because of Upregulation of Cxcr4

(A) Cy/G injection and tissue analysis schedule.

(B) HSC (ckit^{+}Lin^{-}Sca1^{+}Flk2^{-} cells) expansion in the BM in response to Cy/G was normal in *Robo4*$^{-/-}$ mice.

(C) Fewer *Robo4*$^{-/-}$ HSCs relocated to the PB at day 2 of Cy/G treatment. No differences between WT and *Robo4*$^{-/-}$ HSCs were observed at day 4.

(D) The number of MPP (ckit^{+}Lin^{-}Sca1^{+}Flk2^{+} cells) mobilized to the blood was not affected by Robo4 deficiency.

(E) Cxcr4 mRNA levels were significantly higher in *Robo4*$^{-/-}$ HSCs compared to WT HSCs.

(F) *Robo4*$^{-/-}$ HSCs displayed higher Cxcr4 cell surface levels than WT HSCs by flow cytometry analysis. No differences were observed for MPP or myeloid progenitors.

(G) BM stromal (CD45^{-}Ter119^{-}) cells from *Robo4*$^{-/-}$ mice expressed higher levels of Sdf1 than WT stromal cells. Cy/G treatment led to downregulation of Sdf1 in both WT and *Robo4*$^{-/-}$ stromal cells.

(H) Slit2 mRNA levels in BM stromal cells were not affected by loss of Robo4.

(I) Cxcr4 cell surface levels increased on both WT and *Robo4*$^{-/-}$ BM HSCs, but decreased on PB HSCs upon Cy/G treatment.

Data represent at least three (B–G) or two (H and I; n ≥ 10) independent experiments with at least three mice per cohort per experiment (B–D; n ≥ 9). Error bars represent SEM. *p < 0.05; **p < 0.001. See also Figure S3.

NIH-PA Author Manuscript
NIH-PA Author Manuscript
NIH-PA Author Manuscript

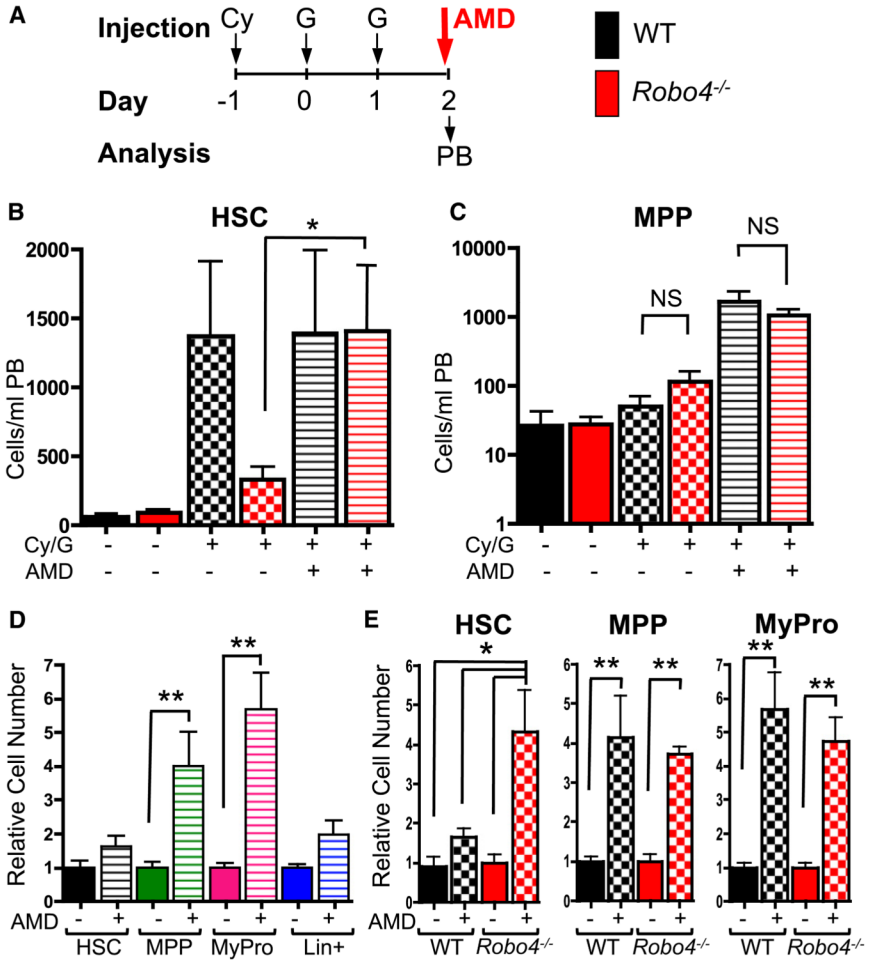

Figure 4. Robo4$^{-/-}$ HSCs Were More Responsive to AMD3100 than Were WT HSCs

(A) Injection and analysis schedule for (B) and (C). PB was analyzed 1 hr after AMD3100 injections on day 2.

(B) *Robo4*$^{-/-}$ HSCs, but not WT HSCs, were mobilized more efficiently by Cy/G +AMD3100 than by Cy/G alone.

(C) Mobilization of MPP was more efficient when AMD3100 was added to the Cy/G treatment. No differences were observed between WT and *Robo4*$^{-/-}$ MPP.

(D) Hematopoietic progenitors were more efficiently mobilized with AMD3100 compared to HSCs. WT mice were subjected to two AMD3100 injections 1 hr apart, with PB analysis 1 hr after the second injection.

(E) *Robo4*$^{-/-}$ HSCs were more efficiently mobilized with AMD3100 compared to WT HSCs. No differences were observed between WT and *Robo4*$^{-/-}$ MPP or myeloid progenitors. Injection and analysis schedule as in (D).

MPP, multipotent progenitors; MyPro, myeloid progenitors (Lin^{-}cKit^{+}Sca1^{-} cells). Error bars represent SEM. Data represent at least three independent experiments with at least three mice per cohort per experiment ($n \geq 9$). *$p < 0.03$; **$p < 0.01$. See also Figure S4.

NIH-PA Author Manuscript

NIH-PA Author Manuscript

NIH-PA Author Manuscript

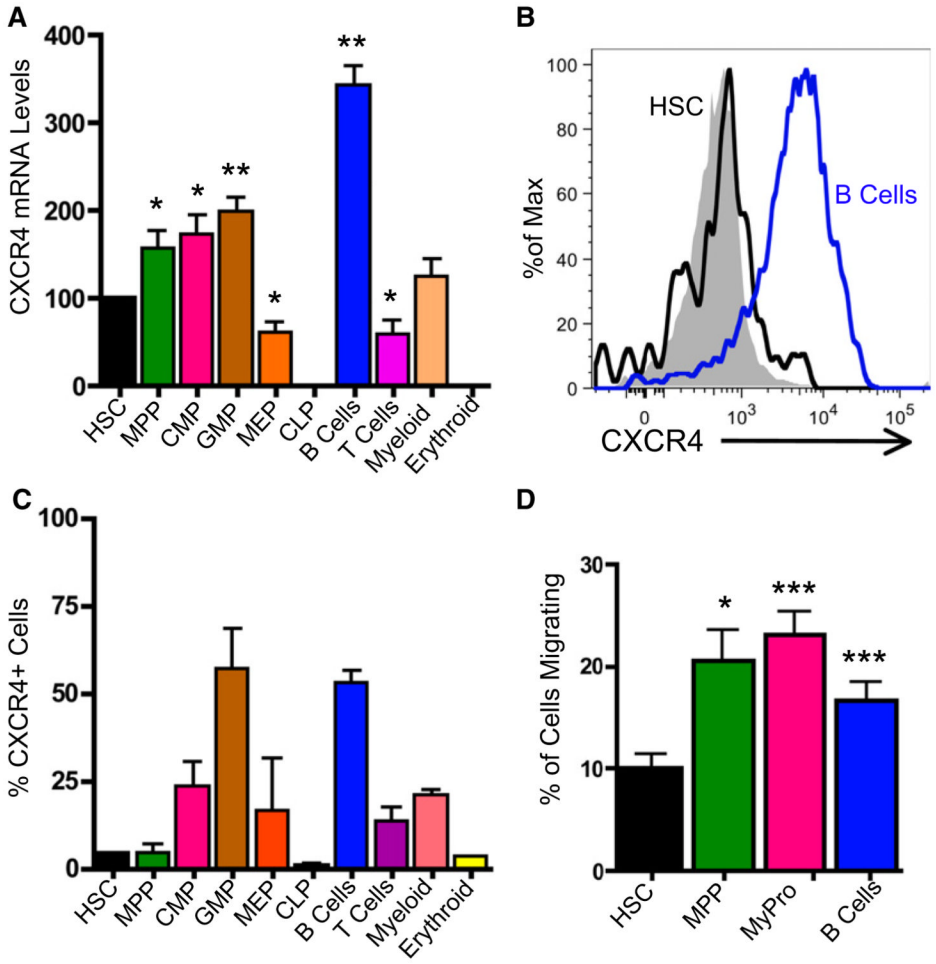

Figure 5. HSCs Expressed Lower Levels of Cxcr4 and Migrated Less Efficiently toward Sdf1 Compared to More Mature Hematopoietic Subpopulations

(A–C) HSCs expressed relatively low levels of Cxcr4 by (A) qRT-PCR analysis and (B, C) flow cytometry cell surface staining.

(D) Transwell migration assays revealed that HSC migration efficiency toward Sdf1 was lower than that of cells expressing higher levels of Cxcr4.

Data represent at least three independent experiments. Error bars represent SEM. *$p < 0.03$; **$p < 0.0001$; ***$p < 0.00001$. See also Figure S5.

NIH-PA Author Manuscript

NIH-PA Author Manuscript

NIH-PA Author Manuscript

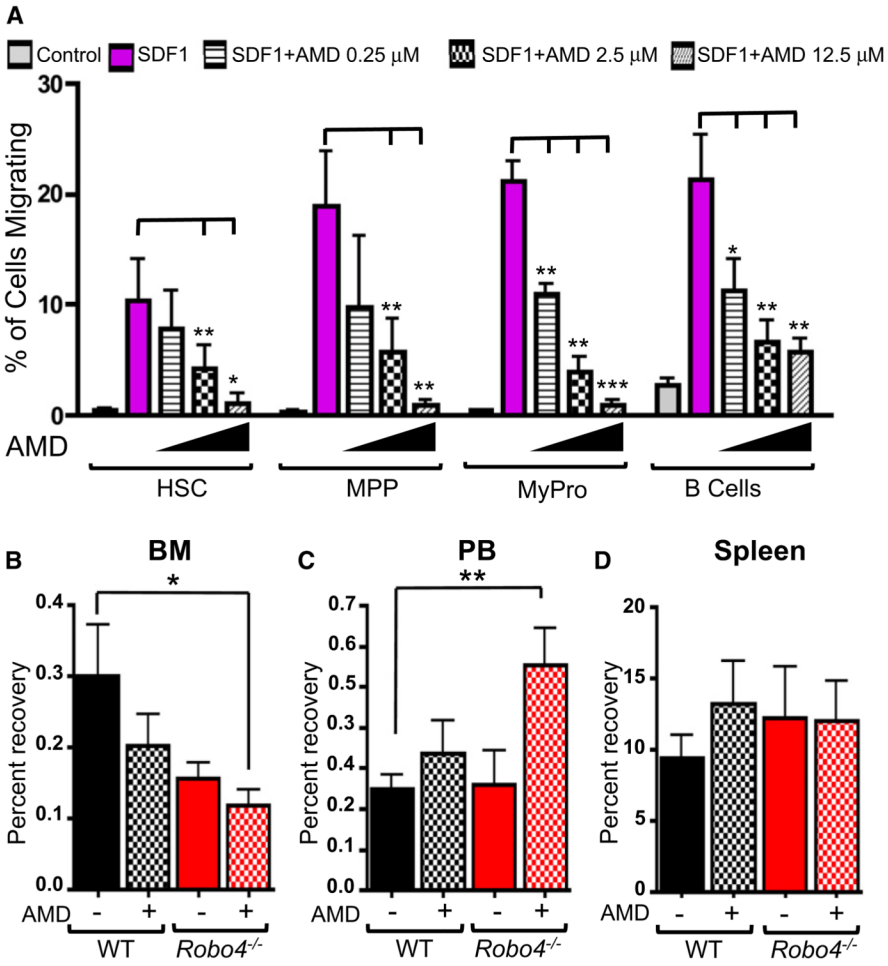

Figure 6. Combined Loss of Robo4 and Cxcr4 Function Impaired HSC Localization to the BM after Transplantation

(A) Preincubation of cells with increasing amounts of AMD3100 inhibited migration toward Sdf1 in vitro.

(B) Fewer HSCs localized to the BM 3 hr after transplantation when Robo4 and/or Cxcr4 function was blocked. CFSE-labeled cells from WT and *Robo4*$^{-/-}$ mice with and without AMD3100 preincubation were injected i.v. into lethally irradiated recipients, followed by tissue analysis for CFSE-positive cells 3 hr later.

(C) A reciprocal increase of *Robo4*$^{-/-}$ and AMD3100-treated HSCs was detected in PB 3 hr after transplantation.

(D) No significant differences in localization to the spleen were detected.

Data represent three independent experiments with three to four mice per cohort per experiment ($n \geq 9$). Error bars represent SEM. *$p < 0.03$; **$p < 0.003$; ***$p < 0.0001$. See also Figure S6.

NIH-PA Author Manuscript

NIH-PA Author Manuscript

NIH-PA Author Manuscript

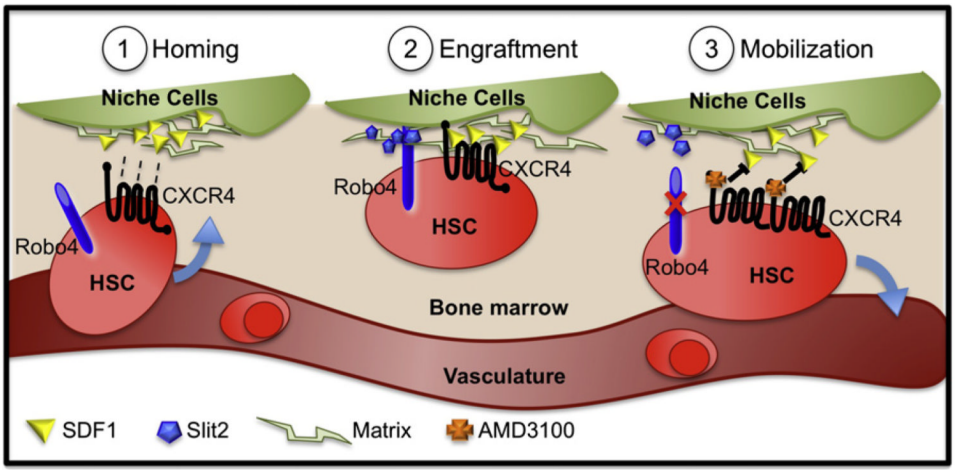

Figure 7. Simplified Model of Robo4- and Cxcr4-Mediated Control of HSC Migration, Engraftment, and Mobilization

During developmental transition of HSC location from fetal liver to BM, or upon transplantation, HSCs home toward BM niches by the attractant cues between Cxcr4 and stromal-derived Sdf1. Adhesive interactions provided by both Cxcr4 and Robo4 promote stable interactions with the niche with long-term engraftment as a result. B cells and other cells expressing high levels of Cxcr4 also home to the BM, but, similar to *Robo4*$^{-/-}$ HSCs, fail to engage in stable niche interactions. AMD3100-induced mobilization of HSCs into the bloodstream is more efficient when Robo4 is deleted, in spite of increased levels of Cxcr4.